Gallium Maltolate Disrupts Tumor Iron Metabolism and Retards the Growth of Glioblastoma by Inhibiting Mitochondrial Function and Ribonucleotide Reductase

Christopher R. Chitambar[1], Mona M. Al-Gizawiy[2], Hisham S. Alhajala[1], Kimberly R. Pechman[3], Janine P. Wereley[1], Robert Wujek[2], Paul A. Clark[4], John S. Kuo[4], William E. Antholine[5], and Kathleen M. Schmainda[2,5]

Abstract

Gallium, a metal with antineoplastic activity, binds transferrin (Tf) and enters tumor cells via Tf receptor1 (TfR1); it disrupts iron homeostasis leading to cell death. We hypothesized that TfR1 on brain microvascular endothelial cells (BMEC) would facilitate Tf-Ga transport into the brain enabling it to target TfR-bearing glioblastoma. We show that U-87 MG and D54 glioblastoma cell lines and multiple glioblastoma stem cell (GSC) lines express TfRs, and that their growth is inhibited by gallium maltolate (GaM) *in vitro*. After 24 hours of incubation with GaM, cells displayed a loss of mitochondrial reserve capacity followed by a dose-dependent decrease in oxygen consumption and a decrease in the activity of the iron-dependent M2 subunit of ribonucleotide reductase (RRM2). IHC staining of rat and human tumor-bearing brains showed that glioblastoma, but not normal glial cells, expressed TfR1 and RRM2, and that glioblastoma expressed greater levels of H- and L-ferritin than normal brain. In an orthotopic U-87 MG glioblastoma xenograft rat model, GaM retarded the growth of brain tumors relative to untreated control ($P = 0.0159$) and reduced tumor mitotic figures ($P = 0.045$). Tumors in GaM-treated animals displayed an upregulation of TfR1 expression relative to control animals, thus indicating that gallium produced tumor iron deprivation. GaM also inhibited iron uptake and upregulated TfR1 expression in U-87 MG and D54 cells *in vitro*. We conclude that GaM enters the brain via TfR1 on BMECs and targets iron metabolism in glioblastoma *in vivo*, thus inhibiting tumor growth. Further development of novel gallium compounds for brain tumor treatment is warranted. *Mol Cancer Ther; 1–11. ©2018 AACR.*

Introduction

Glioblastoma is a primary brain tumor with a dire prognosis. Despite treatment, the median survival of patients with this disease is 14.6 months; few patients survive beyond 2 years from diagnosis (1). The need to develop new therapies for this malignancy is obvious. In this regard, drugs directed at disrupting pathways involved in tumor growth are emerging (2). Recent evidence indicates that iron metabolism and iron-dependent tumor growth are promising targets for cancer treatment as tumor cells have an increased demand for iron to support ribonucleotide reductase activity and mitochondrial function (3). Moreover, iron is required for the activity of certain cyclins and for signaling through the mTOR and WNT pathways (4). A change in the balance of proteins that regulate the cellular intake, storage, and export of iron [transferrin receptor (TfR1), ferritin, and ferroportin, and hepcidin, respectively] in tumors leads to an expanded intracellular iron pool to support iron-dependent malignant cell growth (5). It has been shown that iron homeostasis and iron transport are altered in brain tumors relative to nonmalignant cells (6, 7). Iron, as Tf-Fe, enters the brain by TfRs present on the luminal surface of brain microvascular endothelial cells (BMEC) of the blood–brain barrier (BBB; ref. 8).

Gallium nitrate, a simple metal salt that targets iron metabolism, has clinical antineoplastic activity in bladder cancer and lymphoma (9). It shares certain chemical properties with iron that enables its binding to transferrin (Tf), the transport protein for iron in the circulation (10). Gallium enters cells via TfR1-mediated endocytosis and blocks TfR1-mediated uptake of Tf iron by cells (11). Within the cell, gallium disrupts iron-dependent tumor growth and induces cell death (11).

The antineoplastic activity of gallium nitrate has prompted the development of newer gallium compounds with complex ligand structures. These agents hold the promise of greater clinical efficacy and fewer side-effects (9). For example, gallium maltolate [[(tris-hydroxy-2-methyl-4H-pyran-4-onato)gallium] (GaM) displays greater cytotoxicity than gallium nitrate in lymphoma cell lines and inhibits the growth of lymphoma cells that are resistant to the cytotoxicity of gallium nitrate (12). GaM also inhibits the growth of human T-cell lymphoma xenografts in nude mice confirming its antitumor activity both *in vitro* and *in vivo* (13).

[1]Department of Medicine, Medical College of Wisconsin, Milwaukee, Wisconsin. [2]Department of Radiology, Medical College of Wisconsin, Milwaukee, Wisconsin. [3]Department of Neurosurgery, Medical College of Wisconsin, Milwaukee, Wisconsin. [4]Department of Neurological Surgery, University of Wisconsin School of Medicine and Public Health, Madison, Wisconsin. [5]Department of Biophysics, Medical College of Wisconsin, Milwaukee, Wisconsin.

Corresponding Author: Christopher R. Chitambar, Division of Hematology and Oncology, Medical College of Wisconsin, 9200 W. Wisconsin Avenue, Milwaukee, WI 53226. Phone: 414-805-4600; Fax: 414-805-4606; E-mail: chitambr@mcw.edu

Glioblastomas have a high requirement for iron (14). As iron is taken up by cells through TfR1-mediated endocytosis and TfRs are highly expressed on the surface of glioblastoma cells (15), targeting cellular iron metabolism represents an attractive interventional strategy in glioblastoma therapy. Considering that gallium uses the transport and cellular uptake systems for iron, we hypothesized that GaM can cross the BBB via TfRs on BMECs and target TfR-bearing glioblastoma cells. In this study, we show that GaM inhibits glioblastoma cell growth *in vitro* and *in vivo*. GaM's mechanisms of action include inhibition of cellular iron uptake, disruption of mitochondrial function, and inhibition of RRM2 activity in glioblastoma cells. These findings open the door for further development of gallium-based compounds for glioblastoma treatment.

Materials and Methods

Materials

GaM was provided by Titan Pharmaceuticals. Mouse anti-human TfR antibody (anti-CD71) and rabbit anti-rat TfR antibody were from Biogenex Laboratories, and ABBIOTEC, respectively. Antibodies to RRM2, H- and L-ferritin, and TfR1 were purchased from Santa Cruz Biotechnology Inc. Human Tf, 3-(4,5-Dimethylthiazol-2-yl)-2,5-diphenyltetrazolium bromide (MTT), oligomycin, carbonilcyanide 4-(trifluoromethoxy)phenylhydrazone (FCCP), and antimycin A were obtained from Sigma Chemical Company. Alzet mini-pumps were obtained from Durect Corporation. ^{125}I-Na and ^{55}FeCl$_3$ were purchased from Perkin Elmer and ^{125}I-Tf and ^{55}Fe-Tf were prepared as previously described (16).

Cells

Tissue culture media and supplements were purchased from Life Technologies, unless stated otherwise. All cell lines used were validated at their point of origin. Human glioblastoma U-87 MG and D54 cell lines were obtained from ATCC and courtesy of Dr. D. Bigner (Duke University Medical Center, Durham, NC), respectively. The U-87 MG cells were grown in MEM with Earle's salts fortified with 10% FBS, and supplemented with 1% sodium pyruvate and 0.1% gentamicin. D54 cells were grown in improved MEM with Zn option, fortified with 10% FBS, and supplemented with 0.1 % gentamicin. Human BMECs were a generous gift from Dr. Daniel Kosman (University of Buffalo, Buffalo, NY) and have been described previously (17). The glioblastoma stem cells (GSC) were developed from human glioblastoma and were authenticated, as described previously (18). Experiments were conducted with GSC lines designated GSC-22, GSC-33, and GSC-44. These cells were maintained as neurospheres in a serum-free stem cell culture medium (18, 19).

Interaction of transferrin with GaM

The interaction of Tf with GaM was examined by UV–Vis spectroscopy, as described by Harris and Pecoraro (10). Individual absorbance spectra of human Tf (12.5 µmol/L) and GaM (25 µmol/L) in water were obtained using a Varioskan Flash Spectral Scanning Multimode Reader (Thermo Fisher Scientific Inc.). GaM was added incrementally to the Tf-containing cuvette to achieve final Ga concentrations of 25, 50, and 100 µmol/L, respectively. Absorbance spectra were obtained at room temperature for 10 minutes after the addition of each concentration of GaM to the cuvette.

Cellular Tf binding and internalization

^{25}I-Tf–specific binding to intact cells was measured as reported previously (20). For Tf internalization kinetics, cells were first incubated at 4°C to allow for ^{125}I-Tf binding to cell surface TfR1 and then washed to remove unbound ^{125}I-Tf. Warm medium (37°C) was added to the cells to initiate TfR1 cycling and the fraction of acid-resistant, cell-associated ^{125}I-Tf (representing internalized ^{125}I-Tf) was measured at different time points.

Cellular proliferation

The effect of GaM on cell proliferation was measured by MTT cytotoxicity assay in 96-well microwell plates using an ELX 808 Ultra Microplate Autoreader (Biotech Instruments; ref. 12).

Cellular bioenergetics

The effect of GaM on cellular bioenergetic function was assessed by measuring the oxygen consumption rate (OCR, a measure of oxidative phosphorylation) in intact cells using a Seahorse 96XF Analyzer (Agilent Technologies), according to the manufacturer's directions. Seahorse XF analyzer methodology is reviewed by Dranka and colleagues (21). D54 cells were plated in fresh medium in a 96-well plate (10^4 cells per well) and incubated without additives at 37°C in a CO$_2$ incubator. After 24 hours of incubation, various concentrations of GaM were added to the wells and the incubation continued for an additional 24 hours. The plate was transferred to an XF Analyzer and basal OCR was measured at three timepoints. This was followed by sequential additions of oligomycin (1 µg/mL), FCCP (1 µmol/L), and antimycin A (10 µmol/L).

Electron paramagnetic resonance spectroscopy

X-band electron paramagnetic resonance spectroscopy (EPR) spectra of U-87 MG cells incubated without or with 100 µmol/L GaM for 24 hours were obtained at 110 K with a Bruker EMX spectrometer located at the Nation Biomedical EPR Center at the Medical College of Wisconsin (Milwaukee, WI). EPR spectra were collected as described previously by us (22).

IHC analysis

TfR1, H-ferritin, L-ferritin, and RRM2 expression in normal brain and glioblastoma, and TfR1 expression in human brain microvascular endothelial cells were examined by IHC staining of tissue samples from surgically resected glioblastoma tumors from patients or from animal experiments. Dead cells in tumor xenografts in GaM-treated animals were identified according to the typical nuclear morphologic changes: pyknosis (nuclear condensation), karyorhexis (nuclear fragmentation), and karyolysis (complete dissolution of the nuclear fragments). Percentage of dead cells was calculated out of a total of 1,000 cells (viable and dead) counted. Human tissue was obtained from the Brain and Spinal Cord Tissue Bank of the Medical College of Wisconsin (Milwaukee, WI). IHC staining with specific primary antibodies was performed on a Dako Autostainer Plus Instrument using the Dako EnVision FLEX High pH Detection Kit protocol. Stained slides were visualized using a Nikon Eclipse 80i microscope equipped with a MicroPublisher 3.3 RTV color video camera (Q Imaging). The images were captured using NIS elements imaging software (Version 7.0, Nikon Instruments, Inc.).

Western blotting

Glioblastoma cells were analyzed for the expression of H-ferritin, L-ferritin, and RRM2 proteins by Western blotting using standard protocols. Protein bands on membranes were identified by primary antibodies followed by horseradish peroxidase–labeled secondary antibody. Membranes were developed in Enhanced Chemiluminescence Western blotting detection solution (Amersham Life Science) and exposed to BioMax film for autoradiography.

Animal experiments

The antineoplastic activity of GaM *in vivo* was examined in an intracranial U-87 MG xenograft rat model described previously by us (23). All protocols were approved by the Institutional Animal Care and Use Committee at the Medical College of Wisconsin (Milwaukee, WI).

Male athymic rats weighing approximately 250 g were anesthetized with an intraperitoneal injection of ketamine (60 mg/kg), acepromazine (0.9 mg/kg), and xylazine (6 mg/kg). Once appropriate anesthetic depth was ascertained, the head was immobilized in a stereotactic device. A 2.5-cm skin incision was made along the midline over the bregma and a 1-mm burr hole was drilled in the skull 1 mm anterior and 2 mm lateral to the bregma on the right side (24). Using a 10-µL gas-tight syringe (Hamilton Company), 2×10^5 U-87 MG cells were implanted into the right frontal lobe at a depth of 3 mm relative to the dural surface. The cells were continuously injected over 5 minutes, after which the needle was left stationary for 5 minutes and then slowly withdrawn over an additional 5 minutes. Afterwards, the skin was closed using 3M Vetbond Tissue Adhesive (3 M Animal Care Products).

Eight days following implantation of tumor cells, and after baseline MRI studies were performed, rats were anesthetized with 2% isoflurane. Using aseptic techniques, a small incision was made over the animal's neck and sharp dissection carried out down to the level of the jugular vein. The vein was skeletonized and each pump's drug release catheter was inserted and secured within the vessel lumen. A subcutaneous pocket was dissected free to hold the implanted Alzet minipump reservoir (Durect Corporation) and then the skin wound closed with sutures.

In clinical trials of gallium nitrate, the greatest antineoplastic activity and least toxicity were seen when the drug was administered by continuous intravenous infusion over 5–7 consecutive days (25). On the basis of this treatment schedule, GaM solution or saline control was administered intravenously through the subcutaneously implanted Alzet minipump to provide a steady delivery of GaM. A dose of 50 mg/kg/day was chosen because this was shown to be well tolerated without significant toxicity in rats (26).

Tumor response after 10 days of GaM therapy was assessed by MRI. The relative change in tumor size on MRI from initiation to completion of GaM treatment measured using RECIST V1.1 criteria, as used in the clinic (27). The change in cerebral blood volume (CBV) was measured as described previously (23).

Statistical analysis

Analysis was conducted on the change in tumor size and CBV (day 18–day 8) between the control group and gallium-treated group of animals with a level of significance as $P = 0.05$ (Mann–Whitney test).

Cellular ^{55}FeTf uptake

The effect of GaM on iron uptake by U87 and D54 cells was measured using ^{55}FeTf, as described previously (28).
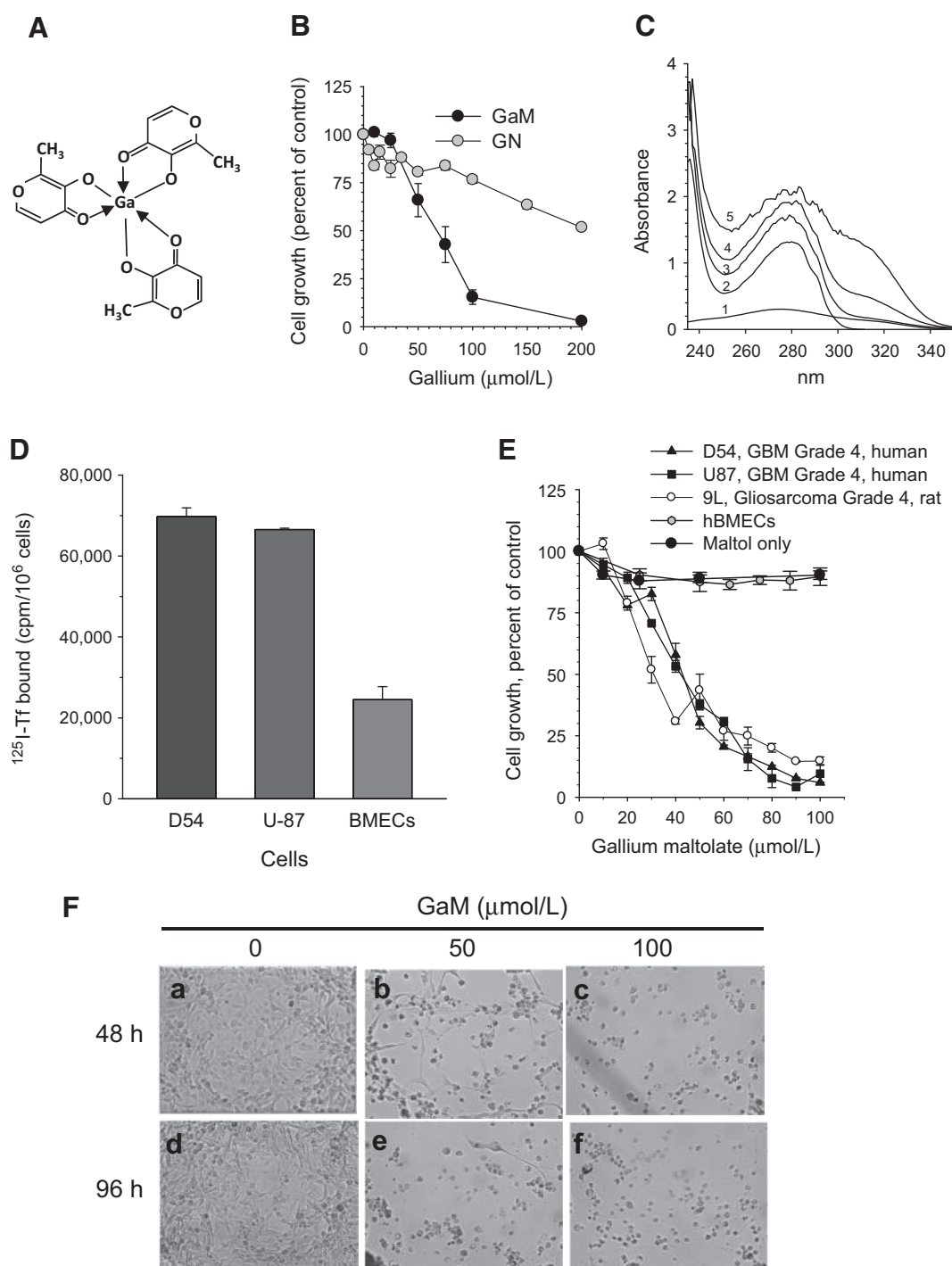
Results

Interaction of Tf with GaM, cellular TfR1 expression, and GaM cytotoxicity in glioblastoma cells

GaM is composed of three maltolate ligands bound to a central gallium atom in a propeller-like arrangement (Fig. 1A; ref. 29). At equimolar gallium concentrations, GaM proved to be more cytotoxic to D54 glioblastoma cells than gallium nitrate (Fig. 1B). This suggests that, in contrast to gallium nitrate, lower concentrations of gallium as GaM are needed to inhibit tumor growth. Accordingly, GaM would be expected to display less toxicity to normal cells than gallium nitrate.

Early studies in animals confirmed that ^{67}Ga citrate injected intravenously was bound entirely to Tf in the circulation (30) and that ^{67}Ga uptake by cells occurred primarily through cell surface TfR1-mediated uptake of Tf-Ga (31). As the binding of gallium to Tf alters the UV-Vis spectra for Tf (10), we examined whether GaM interacted with Tf by measuring changes in the individual UV-Vis spectra of Tf and GaM, and Tf mixed with GaM. As shown in Fig. 1C, a progressive spectral shift was seen when GaM was added to Tf at different ligand to metal ratios, indicating an interaction between GaM and Tf. Whereas the major shift in the spectral peak suggestive of GaM–Tf interaction was seen at ≥280 nm, an increase in the absorbance of Tf at 240–250 nm was also noted when it was incubated with GaM. The latter may be due to the binding of gallium (independent of GaM) to Tf, as the formation of Tf-Ga is known to produce an increase in the absorbance of Tf at 242 nm (10). Hence, it is possible that in solution a small amount of gallium may dissociate from GaM to bind Tf.

As Tf-Ga is preferentially taken up by TfR-bearing cells (11), TfR1 expression on these cells and on BMECs was assessed by ^{125}I-Tf-TfR binding assay. As shown in Fig. 1D, both D54 and U-87 MG cells expressed higher levels of specific Tf binding relative to BMECs, which displayed 63%–65% lower Tf binding. These results suggest that TfRs on glioblastoma cells can be preferentially targeted by Tf-Ga.

To mimic the treatment schedule of gallium nitrate used in clinical trials where the drug is administered continuously for 5–7 days (25), GaM was incubated with human glioblastoma cells for 5 days and the effect on cell proliferation examined. As shown in the dose–response curves in Fig. 1E, GaM inhibited the growth of glioblastoma cells in a dose-dependent manner. In contrast, it was not cytotoxic to human BMECs, thus illustrating a significant differential in GaM's cytotoxicity toward glioblastoma when compared with normal cells. Maltol alone did not inhibit cell proliferation (Fig. 1E). GaM-induced cell death was confirmed by direct visualization of cells (Fig. 1F). D54 cells incubated with 50 and 100 µmol/L GaM for 48 and 96 hours displayed morphologic changes of nuclear condensation and cellular fragmentation consistent with cell death (Fig. 1F, b and c, e and f) compared with control cells that grew normally (Fig. 1F, a and d). In other experiments, the GaM-containing culture medium was removed from the wells after 5 days of incubation and replaced with fresh medium lacking GaM. Incubation was then continued for an additional 5 days and cell growth assessed. Under these conditions, GaM-treated cells failed to regain their ability to proliferate.

Figure 1.
GaM interaction with transferrin (Tf), Tf binding to cells, and effect of GaM on cell growth. **A,** Chemical structure of GaM. **B,** Comparison of the growth-inhibitory effects of GaM and gallium nitrate (GN). D54 cells were incubated with equimolar concentrations of gallium as either GaM or GN. Cell proliferation was measured by MTT assay after 72 hours of incubation. Values shown represent the means $\pm$ SE ($n = 3$). **C,** GaM forms complexes with Tf *in vitro*. UV-Vis spectra of 100 μmol/L GaM (spectrum 1), 12.5 μmol/L Tf (spectrum 2), and 12.5 μmol/L Tf incubated with 12, 50, or 100 μmol/L GaM (spectra 3, 4, and 5, respectively). Spectra were obtained at room temperature after a 30-minute incubation of Tf with GaM. **D,** TfR expression on glioblastoma cells and BMECs. Specific ^{125}I-Tf binding to TfR1 on intact cells is shown. **E,** GaM inhibits the growth of glioblastoma cell lines but not human brain microvascular endothelial cells (hBMECs). Maltol alone does not inhibit D54 cell growth. Cell growth was measured by MTT assay after a 5-day incubation of cells with GaM. Values shown represent means $\pm$ SE ($n = 3$). **F,** GaM induces cell death. Photomicrographs showing morphologic changes consistent with GaM-induced cell death in D54 cells incubated without or with GaM for 48 hours (a–c) or 96 hours (d–f), respectively.
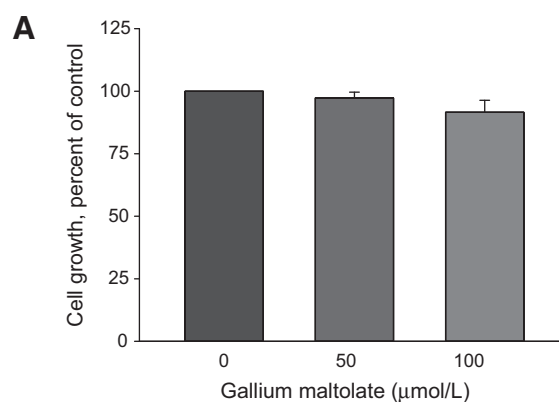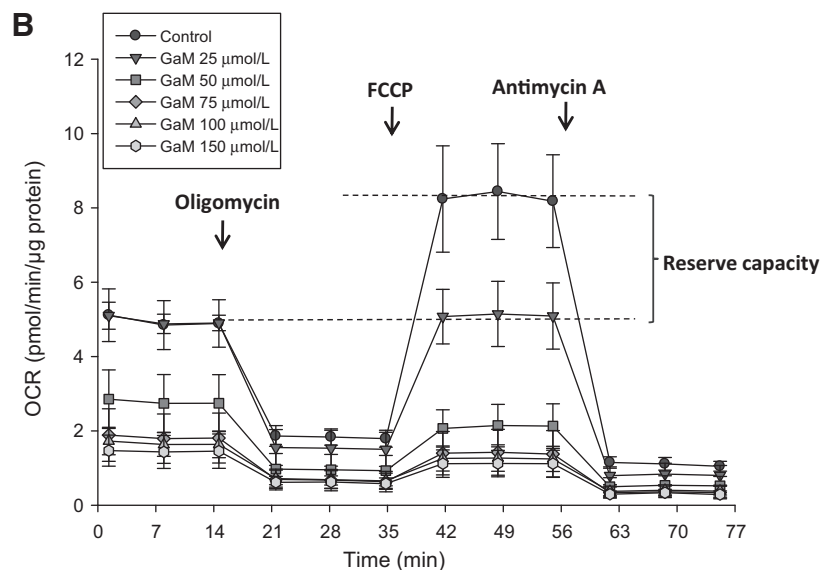
Figure 2.
GaM inhibits mitochondrial bioenergetics. **A,** Effect of GaM on cellular proliferation after a 24-hour incubation. Cellular proliferation in D54 cells was measured by MTT assay. **B,** Effect of GaM on mitochondrial bioenergetics in D54 cells after a 24-hour incubation. Cellular oxygen consumption rate (OCR) was measured by a Seahorse 96XF Analyzer, as described under Materials and Methods.

These latter results strongly suggest that the growth-inhibitory action of GaM is not reversible.

The IC_{50} concentrations for GaM glioblastoma cells *in vitro* are relevant to gallium levels attainable *in vivo*. Tf has two metal-binding sites per molecule and its concentration in the blood is 25.25–45 µmol/L. Under physiologic conditions, approximately one-third of Tf in the circulation is bound by iron thus leaving two-thirds of Tf available to bind Ga. Hence, gallium blood levels of 34–60 µmol/L are possible if these remaining Tf metal-binding sites are occupied by gallium.
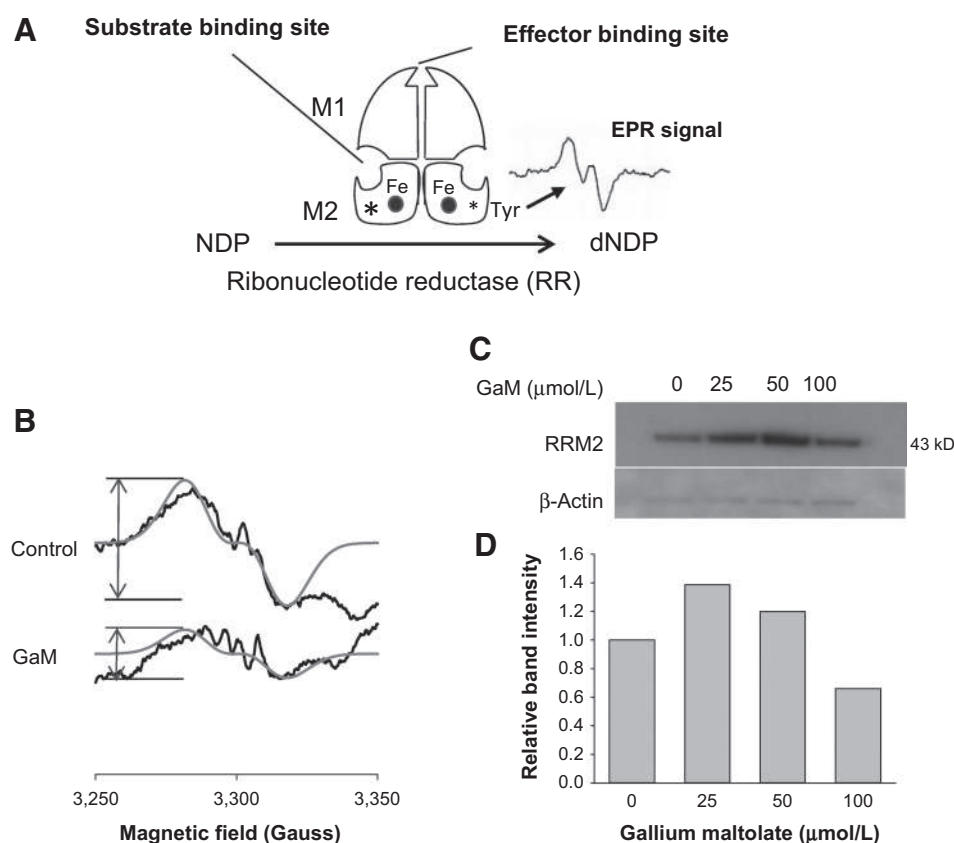
GaM inhibits mitochondrial oxygen consumption

Several proteins of the citric acid cycle and the mitochondrial electron transport chain contain iron–sulfur clusters that are essential for their function. A decrease in cellular iron can therefore result in a loss of mitochondrial function (32, 33). Since we have previously shown that gallium compounds can inhibit cellular iron uptake (28, 34), we examined the effect of GaM on cellular respiration as a measure of mitochondrial function. In these experiments, intact cells were analyzed after they had been incubated with GaM concentrations that were not cytotoxic to cells over 24 hours. As shown in Fig. 2A, D54 cells incubated with 50–100 µmol/L GaM for 24 hours did not display evidence of cell death. However, as shown in Fig. 2B, these cells displayed

a progressive decrease in mitochondrial OCR and a loss of mitochondrial reserve capacity after 24 hours of incubation with increasing concentrations of GaM. Cells incubated with 25 µmol/L GaM, displayed a loss of reserve capacity (also known as the spare respiratory capacity) without a decrease in OCR below baseline, thereby indicating that even low, noncytotoxic concentrations of GaM affected the "fitness" of glioblastoma cells. At higher concentrations, GaM produced a decrease in OCR and reserve capacity. These results suggest that GaM decreases mitochondrial function as an early event before a decrease in cell proliferation or induction of cell death can be detected.

GaM inhibits the iron-dependent activity of RRM2

Ribonucleotide reductase (RR) catalyzes the synthesis of deoxyribonucleotides, a rate-limiting step in DNA synthesis (35). As illustrated in Fig. 3A, RR consists of two heterodimeric subunits M1 and M2, which are under the control of different genes (35). RRM2 expression increases as cells enter S-phase (36). RRM2 contains a binuclear iron center and an EPR-detectable tyrosyl free radical, both of which are essential for its activity (Fig. 3A; ref. 37). Cellular iron deprivation or blockade of iron incorporation into RRM2 inhibits RR enzymatic activity (38). Previously, we showed that gallium nitrate and Tf-Ga inhibit RRM2 activity in leukemia cells by: (i) induction of cellular iron deprivation which limits

Figure 3.
Effect of GaM on the iron-dependent M2 subunit of ribonucleotide reductase (RRM2). **A,** The components of RR. **B,** GaM inhibits the EPR signal of the RRM2 tyrosyl radical. Intact U-87 MG cells incubated without or with 100 μmol/L GaM for 24 hours were analyzed by EPR spectroscopy. EPR spectra of the control and GaM-treated cells (black line); simulated spectra for the tyrosyl radical (gray line), g-2.005, A=53.2 MHz (19 G) for single proton using Easyspin. **C,** RRM2 protein levels in cells incubated with GaM. Cells were analyzed by Western blotting after 24-hour incubation with increasing concentrations of GaM. **D,** Densitometry of the bands shown in **C**.

iron availability to RRM2 (22, 39) and (ii) direct action on enzymatic function which is independent of iron (40). To examine whether GaM interfered with RRM2 in glioblastoma cells, we measured the activity of the RRM2 tyrosyl radical by EPR spectroscopy in intact U-87 MG cells incubated with GaM for 24 hours. As shown in Fig. 3B, the EPR signal in GaM-treated cells was reduced by approximately 65% relative to control cells. To determine whether this was due to a reduction in RRM2 protein, RRM2 expression in U-87 MG cells was analyzed by Western blotting after incubation with GaM for 24 hours. In contrast to the reduction in the RRM2 EPR signal, we found that there was a 1.2- to 1.4-fold increase in RRM2 protein with 25 and 50 μmol/L GaM (Fig. 3C and D). Although the reason for this increase is not obvious, one possible explanation is that cells attempt to compensate for the GaM-induced loss of iron-dependent RR activity by increasing RRM2 protein production. Indeed, an amplification of the *RRM2* gene occurs during the development of drug resistance to hydroxyurea, an agent that blocks RR activity by action on the tyrosyl radical of RRM2 (41). Collectively, these results indicate that GaM decreases the activity of iron-dependent RRM2 without reducing the synthesis of RRM2 protein.

Expression of gallium-targeted iron proteins in normal brain and glioblastoma

To determine whether the expression of iron-related proteins in glioblastoma cells *in vitro* are relevant to glioblastoma *in vivo*, we examined normal and glioblastoma-containing brain tissues from rodent brains for TfR1 and ferritin and from human specimens for RRM2. Consistent with prior reports, we confirmed that TfRs were present on BMECs (Fig. 4A) indicating that these

receptors could serve as portals for GaM to traverse the BBB and enter the brain. Within the brain, TfR1 expression in glioblastoma cells was markedly increased relative to the adjacent normal brain (Fig. 4B). The H- and L-subunits of the iron storage protein ferritin were also increased in glioblastoma (Fig. 4C and D, respectively). Ferritin is composed of 24 subunits of H- and L-ferritin in proportions that differ in various cell types. L-subunit–rich ferritin exists in greater proportion in tissues (such as the liver) that store iron, while H-subunit–rich ferritin exists in greater proportion in metabolically active tissues such as the heart and malignant cells (42). As shown in Fig. 4C and D, both H- and L-ferritin levels were increased in glioblastoma cells relative to normal brain. These findings are consistent with the studies of Schonberg and colleagues, which showed that ferritin levels are elevated in glioblastoma (7).

Figure 4F shows that iron-containing RRM2 protein is highly expressed in human glioblastoma but not in normal brain (Fig. 4E). Collectively, the data in Fig. 4 strongly suggest that glioblastoma cells *in vivo* increase their expression of TfR1 and ferritin to acquire and store greater amounts of iron than the surrounding normal brain in order to support the activity of ribonucleotide reductase and other iron-dependent proteins necessary for tumor proliferation and viability.

GaM retards the growth of glioblastoma in a rodent brain tumor model

Considering that GaM binds to Tf and inhibits the growth of glioblastoma cells *in vitro*, we hypothesized that GaM would enter the brain via TfR1 present on the BMECs of the BBB and inhibit the growth of glioblastoma. Thus, we conducted a proof-of-principle
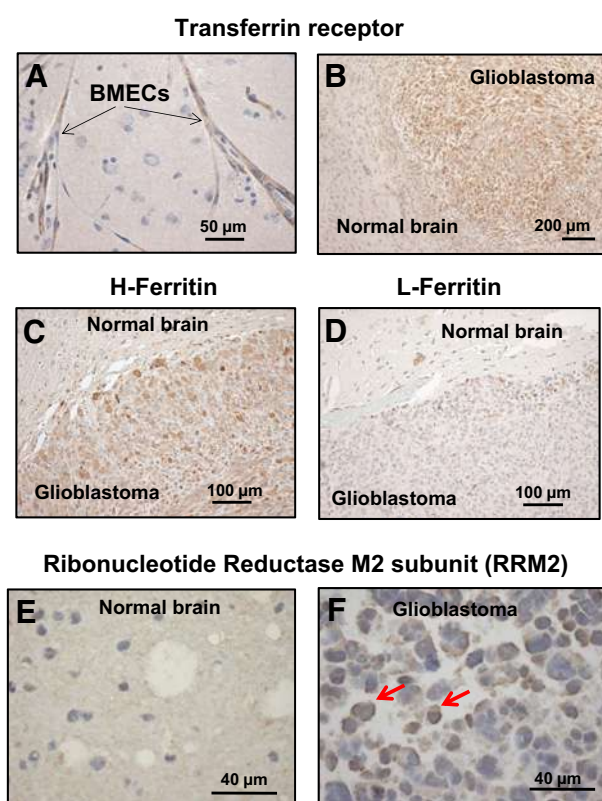
Transferrin receptor

Figure 4.
Transferrin receptor1 (TfR1), ferritin, and ribonucleotide reductase proteins in glioblastoma and normal brain. Proteins were identified by IHC staining. **A,** TfR1 in human brain microvascular endothelial cells (BMECs). **B,** TfR1 in a U-87 MG glioblastoma xenograft inoculated in rat brain. **C** and **D,** H- and L-ferritin in a U-87 MG glioblastoma xenograft inoculated in rat brain. **E,** RRM2 in human normal brain tissue removed therapeutically from a patient with a seizure disorder. **F,** RRM2 in glioblastoma removed from a patient. Red arrows show increased brown staining of RRM2 protein. Increased RRM2 protein is also seen in other malignant cells.

experiment to examine the activity of GaM against glioblastoma in vivo. In the studies shown in Fig. 5, GaM or saline solution (control) was administered to rats inoculated with U-87 MG glioblastoma xenografts in the brain. Treatment of animals with GaM or saline was initiated only after tumors were established in the brain. Tumor response to treatment was assessed by MR imaging and RECIST V1.1 criteria as used in the clinic (27). Figure 5A shows the pre- and posttreatment brain MRI from a representative experiment. Postcontrast T1-weighted images (T1+C) and MION CBV maps were obtained in a glioblastoma xenograft-bearing rat on days 8 and 18 for control (Fig. 5A a–d) and a GaM-treated rat (Fig. 5A e–h). Comparing the cohort of control versus GaM-treated animals, Fig. 5B shows that GaM significantly inhibited the growth of glioblastoma relative to untreated controls. A decrease in CBV in GaM-treated animals was also noted (Fig. 5C); while the difference in this parameter did not reach statistical significance, there was clearly a trend towards a reduction in CBV with gallium treatment.

Tumors were examined for proliferation markers and TfR1 expression. Consistent with the antiproliferative activity of GaM, tumors from GaM-treated animals displayed a significant reduc-

tion in mitotic figures ($P = 0.043$) and mitotic index ($P = 0.045$) compared with untreated tumors (Fig. 5D, a and b). This finding is consistent with an in vivo inhibition of cellular proliferation by GaM in the glioblastoma xenograft and it clearly supports a cytostatic effect of GaM. In addition, GaM-treated tumors displayed a higher percentage of dead cells (37%) than untreated control tumors (24%). Although not significantly different, the observed trend in this parameter suggests that GaM exerts a cytotoxic effect that extends beyond inhibition of proliferation. The conclusion is supported by Fig. 1F and by our prior studies, which show that GaM induces apoptotic cell death in lymphoma cells (12).

GaM inhibits cellular iron uptake and upregulates TfR1 expression in glioblastoma in vitro and in vivo

The expression of TfR1 in tumors from control and GaM-treated animals was measured by IHC after completion of treatment. As shown in Fig. 5E, TfR1 expression was markedly increased in GaM-treated tumors relative to control tumors. This finding is consistent with GaM-induced tumor iron-deprivation in vivo as we have previously shown that Tf-Ga blocks cellular iron uptake and upregulates TfR1 mRNA in human leukemic HL60 cells (43). However, to confirm that glioblastoma U-87 MG and D54 cells would respond to GaM in a similar fashion, we conducted additional experiments which showed that GaM inhibited the uptake of ^{55}Fe-Tf (Fig. 6A and B), and produced an upregulation of TfR1 in both these cell lines (Fig. 6C). These results support our interpretation that the increase in tumor TfR1 expression in GaM-treated animals is secondary to GaM-induced tumor iron deprivation.
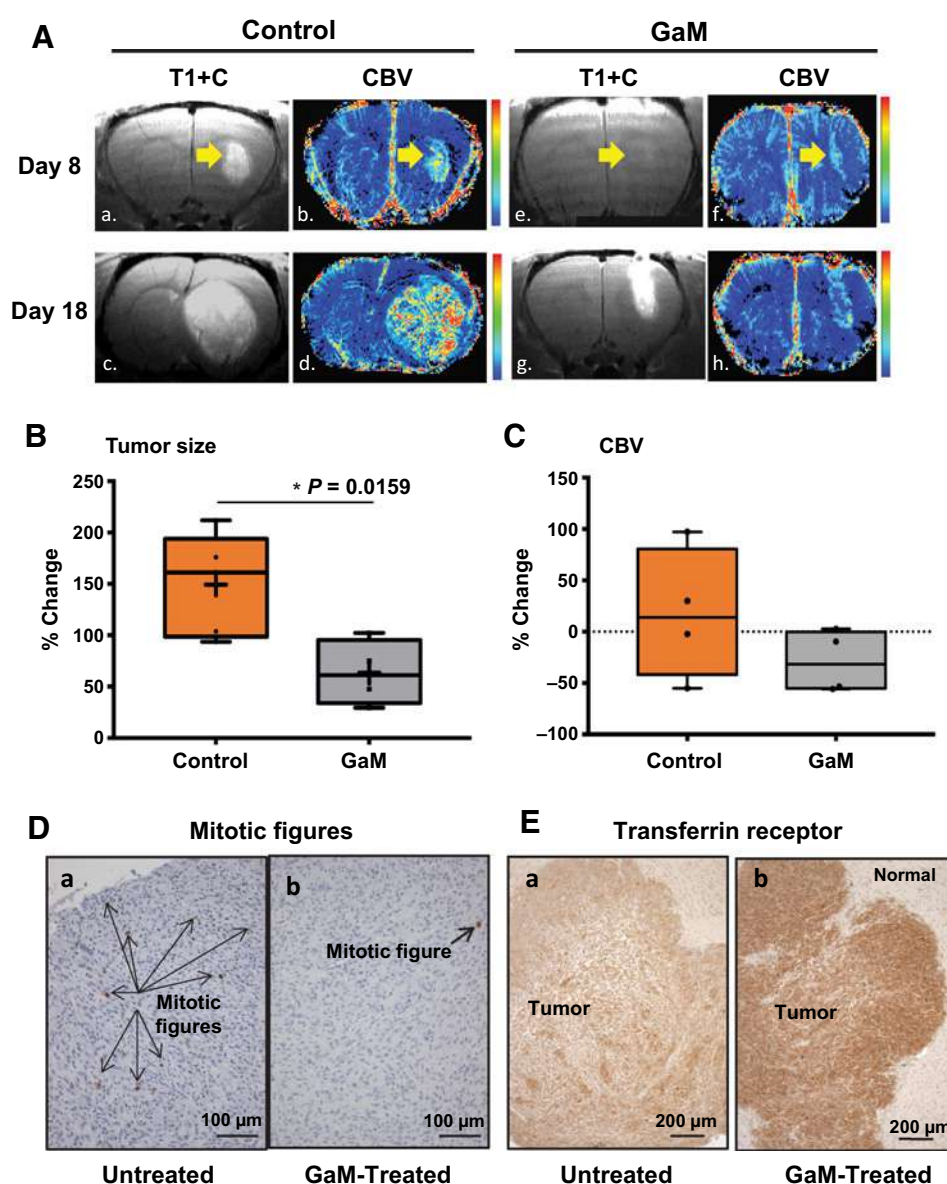
GSCs express ferritin, TfR1, and RRM2, and are sensitive to the cytotoxicity of GaM

As an extension of our studies with U-87 MG and D54 cell lines, we investigated whether three previously described patient-derived GSC lines designated GSC-22, -33, and -44 (19), expressed GaM-targeted iron proteins and were sensitive to its cytotoxicity. Figure 6D shows that all three GSC lines expressed immunoreactive H- and L-ferritin and RRM2 proteins. Ligand–receptor binding and ligand internalization assays confirmed that TfR1 present on GSCs bound ^{125}I-Tf (Fig. 6E) and rapidly internalized it (Fig. 6F). As shown in Fig. 6G, the proliferation of these GSCs could be inhibited by GaM in a dose-dependent manner. Collectively, the experiments studied in Fig. 6D–G indicate GSCs display highly functional TfR1 that can be targeted by GaM.

Discussion

Our study is the first to show that a novel gallium compound, GaM, has antineoplastic activity against glioblastoma in vivo. We demonstrated that GaM inhibited the growth of glioblastoma cell lines in vitro and used MR imaging of the rat brain to measure the impact of GaM on the growth and vascularity of established glioblastoma brain tumor xenografts in live animals. These studies clearly show that GaM significantly retards the growth of tumors and reduces their relative blood volume over a 10-day period of treatment.

Early clinical studies with ^{67}Ga scans showed that ^{67}Ga was taken up by brain tumors (44); additional studies revealed that the cellular uptake and cytotoxicity of gallium was enhanced by Tf (28, 45). Consistent with earlier reports, we confirmed that TfRs

Figure 5.
GaM retards the growth of glioblastoma and alters tumor TfR1 expression *in vivo*. **A,** MR imaging of the brain. Figure shows the postcontrast (T1+C) images and cerebral blood volume (CBV) maps for a control (left: a–d) and a GaM-treated rat (right: e–h) at each imaging time point (day 8 and day 18). **B,** GaM significantly retards the increase in tumor size. Comparison of the percentage change in tumor growth (day 8–16) in the total control ($n = 5$) and GaM-treated ($n = 4$) population. **C,** GaM reduces the change in relative cerebral blood volume (day 8–16). **D,** Mitotic figures are significantly reduced in GaM-treated tumors. **E,** Transferrin receptors (brown staining) are increased in GaM-treated tumors. Tumors from control (untreated) and GaM-treated animals were harvested after completion of treatment and analyzed by IHC for TfR1 expression. Photomicrographs from representative animals are shown.

were expressed on both BMECs and glioblastoma tumors in patients. These findings prompted us to investigate if TfRs could be exploited for the delivery of Tf-Ga to brain tumors.

The strategy of enhancing drug delivery to the brain by conjugating drugs or toxins to Tf or to anti-TfR1 antibodies to target BMEC TfRs has been reported by others (46). However, our approach is different in that we have taken advantage of the high-affinity binding of gallium to endogenous Tf in the circulation to deliver Ga to the brain. We propose that after crossing the BBB, Ga binds Tf in the brain leading to targeting of Tf-Ga- to TfR-bearing glioblastoma cells. It is known that Tf in the normal brain is present in oligodendrocytes and is produced and secreted by the choroidal plexus (47). Furthermore, glioblastoma cells may also secrete Tf as an autocrine growth factor, which may enable them to acquire iron for their growth. *In vitro* studies show that GSCs release Tf to culture medium (7). Thus, Tf in the tumor microenvironment intended to transport iron into TfR1-bearing glio-

blastoma cells could be hijacked by gallium to enhance its uptake by tumor cells. While our studies indicate that GaM penetrates the brain via TfR-mediated transport, it is possible that a variable amount of GaM may also cross the BBB independent of Tf; this is being investigated.

Whereas GaM retards the growth of glioblastoma, it needs to be determined whether gallium compounds will adversely impact on normal brain function. In this regard, it is encouraging to note that central nervous system toxicity was not reported in phase I and II clinical trials of gallium nitrate (25, 26). Also, we did not observe neurologic deficits in the rats treated with GaM. An important consideration is that normal glial cells do not express TfRs *in vivo* (8). Thus, gallium is likely to be taken up by TfR1-expressing glioblastoma cells but not by normal glial tissue. However, neuronal cells do express TfRs (8) and could be targeted by Tf-Ga, but whether this would lead to neuronal toxicity remains to be determined.
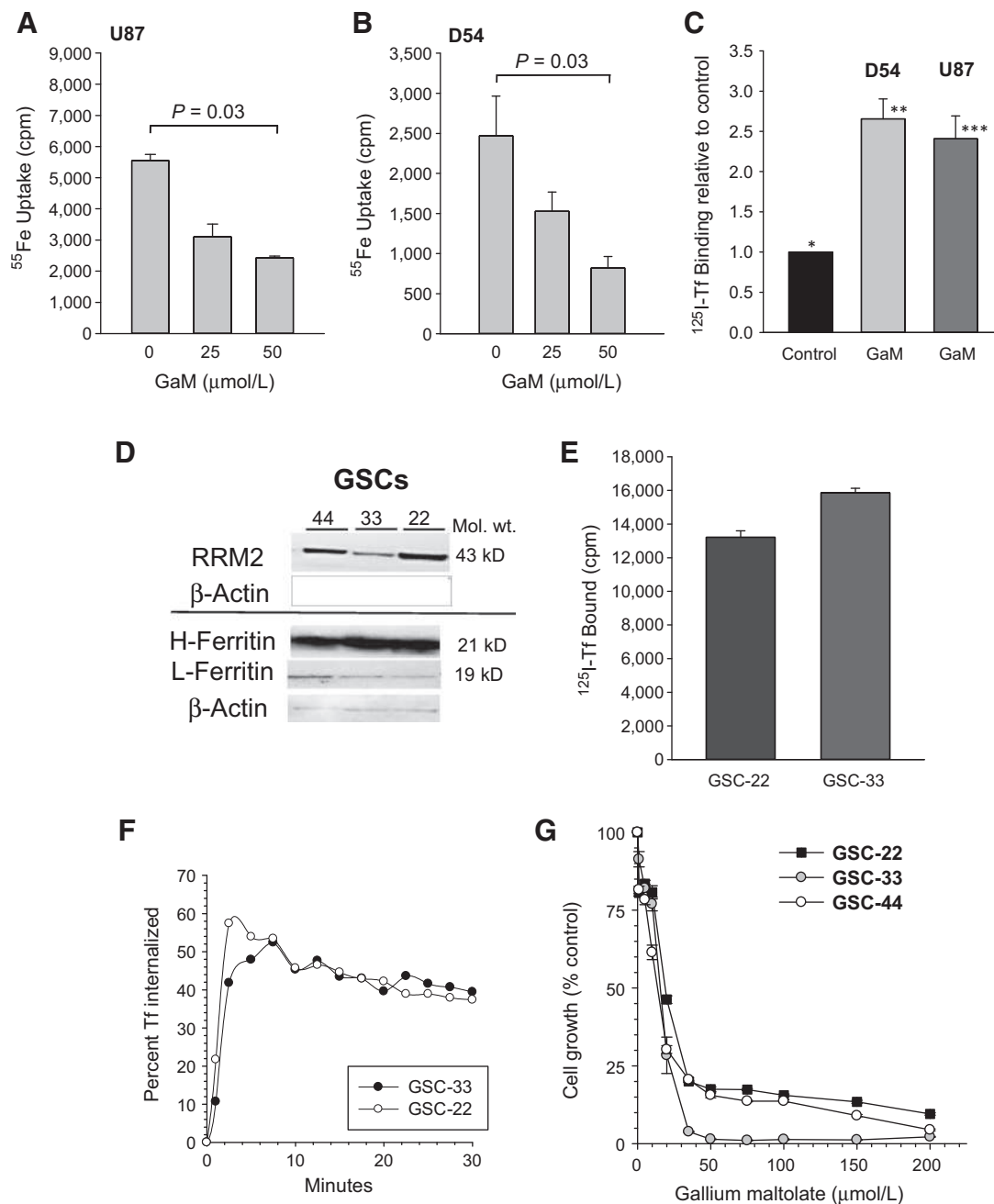
Figure 6.
A–C, GaM inhibits cellular iron uptake and upregulates TfR1 expression in glioblastoma cells. **A** and **B,** [55]Fe uptake by U-87 MG (**A**) and D54 cells (**B**) was measured after cells had been incubated with [55]FeTf for 3 hours in the presence of increasing concentrations of GaM. Values shown are means $\pm$ SE of [55]Fe uptake per 5×10^5 cells. **C,** TfR1 expression in U-87 MG and D54 cells was measured by ^{125}I-Tf binding after a 24-hour incubation of cells with 50 μmol/L GaM. Values shown are means $\pm$ SE of specific ^{125}I-Tf bound per 10^6 cells. Differences between control cells (*, no GaM) and GaM-treated D54 (**) and U87 (***) cells are highly significant ($P = 0.002$, $n = 6$, for D54, and $P = 0.008$, $n = 3$, for U87 cells). **D–F,** Gallium-targeted iron proteins in glioblastoma stem cells (GSC). **D,** Western blot analysis showing ribonucleotide reductase M2 (RRM2) and H- and L-ferritin in GSCs-44, -33, and -22. **E,** TfR1 expression on GSC-22 and -33. **F,** TfR1-mediated internalization kinetics of cell surface TfR-bound ^{125}I-Tf. **G,** Inhibition of GSC cell growth by GaM. Cell proliferation was measured by MTT assay after a 120 hours incubation of cells with GaM.

Collectively, both preclinical and clinical studies suggest a therapeutic index for gallium in which gallium compounds could display antitumor efficacy at concentrations unlikely to affect normal brain cells.

We show that GaM inhibits iron-dependent RRM2 and mitochondrial function. An important point in considering RRM2 as a target in glioblastoma is that normal brain cells do not proliferate *in vivo* and thus would not be expected to express RRM2. In

contrast, glioblastoma being a high-grade proliferating brain tumor would be expected to express RRM2. This was confirmed in our studies comparing the expression of immunoreactive RRM2 protein in glioblastoma versus normal brain. Hence GaM, as an inhibitor of iron-dependent RRM2 activity, would be expected to block DNA synthesis in glioblastoma cells but not in normal brain cells.

Whereas gallium-induced inhibition of RRM2 in itself would be sufficient to inhibit the proliferation of glioblastoma brain tumors, other iron-dependent mechanisms beyond RR could be targeted by gallium. Thus, we focused on GaM's action on the mitochondria. We hypothesized that iron–sulfur cluster–containing proteins of the citric acid cycle and mitochondrial electronic transport chain could be prime targets for disruption by GaM and that this could result in a block in energy production and cell death. We discovered that even at noncytotoxic concentrations, GaM produced loss of cellular reserve capacity in glioblastoma cells. This finding indicates that one of the initial mechanisms of action of GaM on the mitochondria is a loss of its spare respiratory capacity; this could decrease a cell's ability to cope with an energy demand (48). At higher concentrations, GaM further suppressed mitochondrial function as evidenced by a dose-dependent decrease cellular OCR and reserve capacity. This effect undoubtedly contributes to Ga-induced cell death.

Central to gallium's mechanisms of action is its ability to disrupt cellular iron metabolism at several levels (11). Consistent with this mechanism, we found that tumors in GaM-treated rats increased their expression of TfR1. Cellular iron deprivation produces an upregulation of TfR synthesis due to the enhanced interaction of cytoplasmic iron regulatory proteins-1 and -2 (IRPs-1,-2) with iron-regulatory elements (IRE) present on the 3′ untranslated region of the TfR mRNA (49). In support of this mechanism, we demonstrated that GaM inhibited iron uptake by U-87 MG and D54 cells *in vitro* and that this resulted in an increase in cellular TfR expression. Collectively, our studies strongly support tumor iron-deprivation as one of the mechanisms of action of GaM against glioblastoma *in vivo*.

In summary, our results show for the first time that a gallium compound that perturbs tumor iron homeostasis has potential in the therapy of glioblastoma brain tumors. Our animal studies serve as proof-of-principle that GaM can enter the rodent brain

and retard the growth of glioblastoma tumors; this builds the foundation for additional research. Future studies will investigate the efficacy of gallium compounds alone and in combination with other drugs in GSC-derived orthotopic xenograft models. These studies will determine the optimum dose and treatment schedule for gallium compounds and their impact on survival. It is envisioned that such preclinical studies will lead to GaM-based clinical trials in glioblastoma.

Disclosure of Potential Conflicts of Interest
No potential conflicts of interest were disclosed.

Authors' Contributions

References
1. Stupp R, Hegi ME, Mason WP, van den Bent MJ, Taphoorn MJ, Janzer RC, et al. Effects of radiotherapy with concomitant and adjuvant temozolomide versus radiotherapy alone on survival in glioblastoma in a randomised phase III study: 5-year analysis of the EORTC-NCIC trial. Lancet Oncol 2009;10:459–66.
2. Ohka F, Natsume A, Wakabayashi T. Current trends in targeted therapies for glioblastoma multiforme. Neurol Res Int 2012;2012: 878425.
3. Richardson DR, Kalinowski DS, Lau S, Jansson PJ, Lovejoy DB. Cancer cell iron metabolism and the development of potent iron chelators as antitumour agents. Biochim Biophys Acta 2009;1790:702–17.
4. Torti SV, Torti FM. Iron and cancer: more ore to be mined. Nat Rev Cancer 2013;13:342–55.
5. Pinnix ZK, Miller LD, Wang W, D'Agostino R Jr, Kute T, Willingham MC, et al. Ferroportin and iron regulation in breast cancer progression and prognosis. Sci Transl Med 2010;2:43ra56.
6. Hanninen MM, Haapasalo J, Haapasalo H, Fleming RE, Britton RS, Bacon BR, et al. Expression of iron-related genes in human brain and brain tumors. BMC Neurosci 2009;10:36.
7. Schonberg DL, Miller TE, Wu Q, Flavahan WA, Das NK, Hale JS, et al. Preferential iron trafficking characterizes glioblastoma stem-like cells. Cancer Cell 2015;28:441–55.
8. Moos T, Rosengren NT, Skjorringe T, Morgan EH. Iron trafficking inside the brain. J Neurochem 2007;103:1730–40.
9. Chitambar CR. Gallium-containing anticancer compounds. Future Med Chem 2012;4:1257–72.
10. Harris WR, Pecoraro VL. Thermodynamic binding constants for gallium transferrin. Biochemistry 1983;22:292–9.
11. Chitambar CR. Gallium and its competing roles with iron in biological systems. Biochim Biophys Acta 2016;1863:2044–53.
12. Chitambar CR, Purpi DP, Woodliff J, Yang M, Wereley JP. Development of gallium compounds for treatment of lymphoma: gallium maltolate, a novel hydroxypyrone gallium compound induces apoptosis and circumvents lymphoma cell resistance to gallium nitrate. J Pharmacol Exp Ther 2007;322:1228–36.
13. Wu X, Wang TW, Lessmann GM, Saleh J, Liu X, Chitambar CR, et al. Gallium maltolate inhibits human cutaneous T-cell lymphoma tumor development in mice. J Invest Dermatol 2014;135:877–84.

14. Legendre C, Garcion E. Iron metabolism: a double-edged sword in the resistance of glioblastoma to therapies. Trends Endocrinol Metab 2015;26:322–31.

15. Voth B, Nagasawa DT, Pelargos PE, Chung LK, Ung N, Gopen Q, et al. Transferrin receptors and glioblastoma multiforme: current findings and potential for treatment. J Clin Neurosci 2015;22:1071–6.

16. Chitambar CR, Wereley JP. Transferrin receptor-dependent and -independent iron transport in gallium-resistant human lymphoid leukemic cells. Blood 1998;91:4686–93.

17. Stins MF, Badger J, Sik KK. Bacterial invasion and transcytosis in transfected human brain microvascular endothelial cells. Microb Pathog 2001;30: 19–28.

18. Clark PA, Iida M, Treisman DM, Kalluri H, Ezhilan S, Zorniak M, et al. Activation of multiple ERBB family receptors mediates glioblastoma cancer stem-like cell resistance to EGFR-targeted inhibition. Neoplasia 2012; 14:420–8.

19. Zorniak M, Clark PA, Leeper HE, Tipping MD, Francis DM, Kozak KR, et al. Differential expression of 2′,3′ -cyclic-nucleotide 3′-phosphodiesterase and neural lineage markers correlate with glioblastoma xenograft infiltration and patient survival. Clin Cancer Res 2012;18:3628–36.

20. Klausner RD, van Renswoude J, Ashwell G, Kempf C, Schecter AN, Dean A, et al. Receptor-mediated endocytosis of transferrin in K562 cells. J Biol Chem 1983;258:4715–24.

21. Dranka BP, Benavides GA, Diers AR, Giordano S, Zelickson BR, Reily C, et al. Assessing bioenergetic function in response to oxidative stress by metabolic profiling. Free Radic Biol Med 2011;51:1621–35.

22. Narasimhan J, Antholine WE, Chitambar CR. Effect of gallium on the tyrosyl radical of the iron-dependent M2 subunit of ribonucleotide reductase. Biochem Pharmacol 1992;44:2403–8.

23. Pechman KR, Donohoe DL, Bedekar DP, Kurpad SN, Hoffmann RG, Schmainda KM. Characterization of bevacizumab dose response relationship in U87 brain tumors using magnetic resonance imaging measures of enhancing tumor volume and relative cerebral blood volume. J Neurooncol 2011;105:233–9.

24. Pechman KR, Donohoe DL, Bedekar DP, Kurpad SN, Schmainda KM. Evaluation of combined bevacizumab plus irinotecan therapy in brain tumors using magnetic resonance imaging measures of relative cerebral blood volume. Magn Reson Med 2012;68:1266–72.

25. Warrell RP Jr, Coonley CJ, Straus DJ, Young CW. Treatment of patients with advanced malignant lymphoma using gallium nitrate administered as a seven-day continuous infusion. Cancer 1983;51:1982–7.

26. Foster BJ, Clagett-Carr K, Hoth D, Leyland-Jones B. Gallium nitrate: the second metal with clinical activity. Cancer Treat Rep 1988;70:1311–9.

27. Eisenhauer EA, Therasse P, Bogaerts J, Schwartz LH, Sargent D, Ford R, et al. New response evaluation criteria in solid tumours: revised RECIST guideline (version 1.1). Eur J Cancer 2009;45:228–47.

28. Chitambar CR, Seligman PA. Effects of different transferrin forms on transferrin receptor expression, iron uptake and cellular proliferation of human leukemic HL60 cells: mechanisms responsible for the specific cytotoxicity of transferrin-gallium. J Clin Invest 1986;78:1538–46.

29. Bernstein LR, Tanner T, Godfrey C, Noll B. Chemistry and pharmacokinetics of gallium maltolate, a compound with high oral gallium bioavailability. Met Based Drugs 2000;7:33–47.

30. Vallabhajosula SR, Harwig JF, Siemsen JK, Wolf W. Radiogallium localization in tumors: blood binding and transport and the role of transferrin. J Nucl Med 1980;21:650–6.

31. Larson SM, Rasey JS, Allen DR, Nelson NJ, Grunbaum Z, Harp GD, et al. Common pathway for tumor cell uptake of gallium-67 and iron-59 via a transferrin receptor. J Natl Cancer Inst 1980;64:41–53.

32. Oexle H, Gnaiger E, Weiss G. Iron-dependent changes in cellular energy metabolism: influence on citric acid cycle and oxidative phosphorylation. Biochim Biophys Acta 1999;1413:99–107.

33. Yoon YS, Byun HO, Cho H, Kim BK, Yoon G. Complex II defect via down-regulation of iron-sulfur subunit induces mitochondrial dysfunction and cell cycle delay in iron chelation-induced senescence-associated growth arrest. J Biol Chem 2003;278:51577–86.

34. Chitambar CR, Narasimhan J. Targeting iron-dependent DNA synthesis with gallium and transferrin-gallium. Pathobiology 1991;59:3–10.

35. Aye Y, Li M, Long MJ, Weiss RS. Ribonucleotide reductase and cancer: biological mechanisms and targeted therapies. Oncogene 2014;34: 2011–21.

36. Eriksson S, Gräslund A, Skog S, Thelander L, Tribukait B. Cell cycle-dependent regulation of mammalian ribonucleotide reductase. The S phase-correlated increase in subunit M2 is regulated by de novo protein synthesis. J Biol Chem 1984;259:11695–700.

37. Gräslund A, Sahlin M, Sjöberg BM. The tyrosyl free radical in ribonucleotide reductase. Environ Health Perspect 1985;64:139–49.

38. Nyholm S, Mann GJ, Johansson AG, Bergeron RJ, Gräslund A, Thelander L. Role of ribonucleotide reductase in inhibition of mammalian cell growth by potent iron chelators. J Biol Chem 1993;268: 26200–5.

39. Chitambar CR, Matthaeus WG, Antholine WE, Graff K, O'Brien WJ. Inhibition of leukemic HL60 cell growth by transferrin-gallium: effects on ribonucleotide reductase and demonstration of drug synergy with hydroxyurea. Blood 1988;72:1930–6.

40. Chitambar CR, Narasimhan J, Guy J, Sem DS, O'Brien WJ. Inhibition of ribonucleotide reductase by gallium in murine leukemic L1210 cells. Cancer Res 1991;51:6199–201.

41. Wright JA, Alam TG, McClarty GA, Tagger AY, Thelander L. Altered expression of ribonucleotide reductase and role of M2 gene amplification in hydroxyurea-resistant hamster, mouse, rat and human cell lines. Somatic Cell Mol Genet 1987;13:155–65.

42. Torti FM, Torti SV. Regulation of ferritin genes and protein. Blood 2002;99:3505–16.

43. Haq RU, Chitambar CR. Modulation of transferrin receptor mRNA by transferrin-gallium in human myeloid HL60 cells and lymphoid CCRF-CEM cells. Biochem J 1993;294:873–7.

44. Waxman AD, Siemsen JK, Lee GC, Wolfstein RS, Moser L. Reliability of gallium brain scanning in the detection and differentiation of central nervous system lesions. Radiology 1975;116:675–8.

45. Harris AW, Sephton RG. Transferrin promotion of 67Ga and 59Fe uptake by cultured mouse myeloma cells. Cancer Res 1977;37:3634–8.

46. McCarthy RC, Kosman DJ. Mechanistic analysis of iron accumulation by endothelial cells of the BBB. Biometals 2012;25:665–75.

47. Leitner DF, Connor JR. Functional roles of transferrin in the brain. Biochim Biophys Acta 2012;1820:393–402.

48. Respiratory chains. In: Nicholls DG, Ferguson SJ, authors. Bioenergetics. 4th ed. Academic Press, Cambridge, Massachusetts 2013. p. 91–157.

49. Lane DJ, Merlot AM, Huang ML, Bae DH, Jansson PJ, Sahni S, et al. Cellular iron uptake, trafficking and metabolism: key molecules and mechanisms and their roles in disease. Biochim Biophys Acta 2015; 1853:1130–44.